

This is the accepted manuscript made available via CHORUS. The article has been published as:

# Collapse of the electron gas from three to two dimensions in Kohn-Sham density functional theory

Aaron D. Kaplan, Kamal Wagle, and John P. Perdew

Phys. Rev. B **98**, 085147 — Published 28 August 2018

DOI: [10.1103/PhysRevB.98.085147](https://doi.org/10.1103/PhysRevB.98.085147)

# Collapse of the Electron Gas from Three to Two Dimensions in Kohn-Sham Density Functional Theory

Aaron D. Kaplan,<sup>1</sup> Kamal Wagle,<sup>1</sup> and John P. Perdew<sup>1,2</sup>

<sup>1</sup>*Department of Physics, Temple University, Philadelphia, PA 19122*

<sup>2</sup>*Department of Chemistry, Temple University, Philadelphia, PA 19122*

(Dated: August 13, 2018)

Under pressure, a quasi-2D electron gas can collapse toward the true 2D limit. In this limit, the exact exchange-correlation energy per electron has a known finite limit, but general-purpose semilocal approximate density functionals, like the local density approximation (LDA) and Perdew-Burke-Ernzerhof generalized gradient approximation (PBE GGA), are known to diverge to minus infinity. Here we consider a model density for a non-interacting electron gas confined to a thickness  $L$  by infinite-barrier walls, with a fixed 2D density  $1/(\pi(r_s^{2D})^2)$ , and  $r_s^{2D} = 4$  Bohr. We estimate that LDA, PBE, and the strongly constrained and appropriately normed (SCAN) meta-GGA are accurate for the exchange-correlation energy over a wide quasi-2D range,  $1.5 < L/r_s^{2D} < 3.85$ , but not for smaller  $L$ . Of these functionals, only SCAN tends to a finite limit when  $L$  tends to 0. Since the non-interacting kinetic energy, treated exactly in Kohn-Sham theory, dominates in this limit within a deformable jellium model, all of the general-purpose functionals can estimate the pressure required to achieve any thickness (with SCAN and LDA better than PBE). This pressure vanishes around  $L/r_s^{2D} = 3.85$ , where the 3D electron density is roughly that of the valence electrons in metallic potassium, and reaches about 20 GPa at  $L/r_s^{2D} = 1.5$  and 400 GPa at  $L/r_s^{2D} = 0.6$ .

## I. INTRODUCTION

Ground state Kohn-Sham density functional theory (KS-DFT)<sup>1</sup> is a widely used method to find accurate approximate properties of many-electron systems at reasonable computation cost. The ground state energy in DFT is the sum of non-interacting kinetic, electrostatic, and exchange-correlation energy terms.

All three are exact in principle, however in practice the exchange-correlation energy  $E_{xc}$  must be approximated.  $E_{xc}$  is often decomposed into exchange  $E_x$  (Pauli exclusion) and correlation  $E_c$  (driven by Coulomb repulsion) terms. Most of the chemical bonding energy is due to exchange-correlation energy<sup>2</sup>, therefore reliable approximations of  $E_{xc}$  are needed to reach chemical accuracy. These approximations have a hierarchy, sometimes referred to as the Jacob's Ladder of density functional approximations<sup>3</sup>.

In order of increasing accuracy, they are the local density approximation (LDA)<sup>1,4</sup> (e.g. Ref. 5), generalized gradient approximation (GGA, e.g. Ref. 6), meta-GGA (e.g. Ref. 7), and fully-nonlocal hyper-GGA<sup>3</sup>. The LDA exchange-correlation energy density is constructed from the local electron density alone, while the GGA adds the gradient of the density, the meta-GGA adds the non-interacting orbital kinetic energy density, and the hyper-GGA adds the one-matrix (as in the exact  $E_x$ )<sup>2</sup>. The first three rungs of this ladder of approximations are the computationally-efficient semilocal functionals, and other functionals are typically fully nonlocal.

More recently, Sun, Ruzsinszky, and Perdew<sup>7</sup> designed a meta-GGA to satisfy all 17 known exact constraints that a meta-GGA can. The strongly-constrained and appropriately normed (SCAN) functional has been shown to be accurate for diverse systems: ice<sup>8</sup>, high- $T_c$  cuprate superconductors<sup>9</sup>, metallic surfaces<sup>10</sup>, water<sup>8,11</sup>, solids<sup>12</sup>,

structural phase transitions<sup>13</sup>, and more.

The present work considers only the general-purpose non-empirical functionals LDA<sup>1,5</sup>, PBE<sup>6</sup> (GGA), and SCAN<sup>7</sup> (meta-GGA) functionals, all of which benefit from error cancellation in their approximations to  $E_{xc}$ . Error cancellation is best understood in terms of the exchange-correlation hole, the region of density depletion around an electron<sup>14,15</sup>. The exchange-correlation hole is deeper and shorter-ranged than the exchange hole, and thus less fully nonlocal<sup>16</sup>. While the exact exchange-correlation hole is typically non-spherical, Gunnarsson and Lundqvist<sup>17</sup> argued that an approximate  $E_{xc}$  only depends upon the spherical average of the exchange-correlation hole.

Our last diversion before discussing the system in question is nonuniform scaling in one coordinate. For  $c$  a constant, a non-uniformly scaled density has the form

$$n_c^x(x, y, z) = c n(cx, y, z). \quad (1)$$

Exact constraints on the exchange and correlation functionals under nonuniform scaling are known<sup>18</sup>.  $E_x$  and  $E_c$  from SCAN are designed to approach finite values under nonuniform scaling as  $c \rightarrow \infty$ <sup>7</sup>. Neither LDA nor PBE are constrained to finite values in this limit.

This brings us to the problem at hand, the quasi-two dimensional (2D) electron gas. This is an electron gas confined to a well that is infinite in two dimensions, and finite in the third. The quasi-2D electron gas can be used to model semiconductor devices<sup>19–21</sup> and quantum dots<sup>20</sup>. DFT was first applied to this system by Ryan<sup>19</sup> to study the collective electron oscillations of a semiconductor quasi-2D well (MOSFET).

Kim *et al.*<sup>20</sup> were the first to study the 2D limit of the quasi-2D electron gas. They found that the LDA, a GGA, and a meta-GGA were not able to recover a finite value, however the average density approximation (a fully

nonlocal functional) was able to recover a finite limit. In LDA, GGA, and meta-GGA, the exchange energy per electron is an average over the 3D electron density  $n$  of  $-fn^{1/3}$ , where  $f$  is a positive function. Unless  $f$  goes to zero fast enough, the approximate exchange energy per electron will diverge to minus infinity in the approach to the true 2D limit, because the 3D density diverges. In LDA,  $f$  is a constant. In the PBE GGA,  $f$  approaches a constant that is bigger than the one for LDA by a factor of 1.804. But, in the SCAN meta-GGA,  $f$  more correctly approaches zero.

García-González<sup>21</sup> showed similar results to Kim *et al.*, and demonstrated that the weighted density approximation (another fully nonlocal functional) was also able to recover a finite 2D limit.

The method of this work follows that of Pollack and Perdew<sup>22</sup>, who used nonuniform scaling to study the behavior of density functional approximations for a quasi-2D system. They also discussed the constraints functionals should obey in the 2D limit.

Constantin *et al.*<sup>23</sup> extended the work of Pollack and Perdew to include other hyper-GGAs and the random phase approximation, and found for the considered functionals that only rungs higher than meta-GGA could recover a finite 2D limit. Last, Constantin<sup>24</sup> described modifications to the enhancement factor of a GGA or meta-GGA to recover the exact  $E_{xc}$  of a uniform 2D electron gas.

The challenge that the 2D limit presents to 3D semilocal functionals like LDA, PBE, or SCAN is well understood. For a wide quasi-2D system, the system-averaged exact exchange-correlation hole<sup>14–17</sup> around an electron is not so different from the spherical hole of the 3D uniform electron gas, on which all 3D semilocal approximations are based. But the exact exchange-correlation hole must remain within the electron density. As the width of the quasi-2D system tends to zero (the true 2D limit), the exact hole must flatten into a thin pancake shape. Even the required spherical average<sup>17</sup> of the exact hole cannot be approximated by 3D semilocal functionals in this limit.

## II. MODEL

### A. Solving the Kohn-Sham Equation

What follows is in atomic units,  $\hbar = m = e^2 = 1$ . Let the Kohn-Sham potential for the quasi-2D electron gas be

$$v_s(x, y, z) = \begin{cases} 0, & 0 < x < L \\ \infty, & \text{otherwise} \end{cases}. \quad (2)$$

This defines a well of finite transverse width  $L$ , and infinite planar area. Solving the Kohn-Sham Equation

$$\left(\frac{1}{2}\nabla^2 + v_s - E_i\right)\phi_i = 0 \quad (3)$$

subject to this potential gives the orthonormal KS orbitals for  $0 < x < L$

$$\phi_{\ell, \vec{k}}(x, y, z) = \left[\frac{2}{LA}\right]^{1/2} \sin(\pi\ell x/L) \times \exp[i(k_y y + k_z z)], \quad \ell = 1, 2, 3, \dots \quad (4)$$

where  $A$  is the area of a large square on whose sides we impose periodic boundary conditions, and the  $k_i$  are the components of the planar Bloch wavevector  $\vec{k}$ . This simple model is not intended to be realistic, but only to share fundamental features with more realistic models, in the same way that the uniform electron gas model represents bulk metals and the infinite barrier model<sup>25</sup> represents metal surfaces.

In the quasi-2D, or small  $L$ , regime only the  $\ell = 1$  sub-band is occupied, the other sub-bands being very high in energy. Therefore the ground state density is

$$n(x) = \sum_{\vec{k}, |\vec{k}| < k_F^{2D}} |\phi_{1, \vec{k}}(x, y, z)|^2 = \frac{2}{L\pi(r_s^{2D})^2} \sin^2\left(\frac{\pi x}{L}\right), \quad (5)$$

where  $r_s^{2D}$  is the 2D Seitz radius. The number of electrons per unit area is

$$\int_0^L dx n(x) = \frac{1}{\pi(r_s^{2D})^2} = n_s^{2D}. \quad (6)$$

### B. Assumptions

Following the lead of Pollack and Perdew<sup>22</sup>, we can observe the effect of collapse under nonuniform scaling. The scaled density is

$$n_c^x(x) = \frac{2}{(L/c)\pi(r_s^{2D})^2} \sin^2\left(\frac{\pi x}{L/c}\right), \quad (7)$$

where  $c \geq 1$ . As we shrink the transverse well width  $L$  by increasing the scale factor  $c$ , and keep the number of electrons fixed, the density of electrons within the well increases. Precisely,

$$\lim_{c \rightarrow \infty} n_c^x(x) = \lim_{L \rightarrow 0} n(x) = n_s^{2D} \delta(x), \quad (8)$$

where  $\delta(x)$  is the Dirac delta.

From Görling and Levy<sup>18</sup>, as amended by Pollack and Perdew<sup>22</sup>, we expect the exchange and correlation energies per electron to scale as

$$\begin{aligned} \lim_{L \rightarrow 0} E_x/N &> -\infty \\ \lim_{L \rightarrow 0} E_c/N &> -\infty. \end{aligned} \quad (9)$$

LDA and PBE do not satisfy the first constraint. PBE satisfies the second constraint, while LDA does not. SCAN was designed to constrain  $E_x/N$  and  $E_c/N$  to finite values under nonuniform scaling. Thus, we expect  $E_{xc}^{\text{SCAN}}/N$  to approach a finite value as  $L \rightarrow 0$ .

The quasi-2D range of thicknesses  $L$  is

$$\sqrt{3/2}\pi r_s^{2D} = L_{\max} > L > 0. \quad (10)$$

$L_{\max}$  is found by demanding<sup>22</sup>

$$E(\ell = 1, |\vec{k}| = k_F^{2D}) < E(\ell = 2, |\vec{k}| = 0), \quad (11)$$

i.e., the highest occupied orbital in the  $\ell = 1$  sub-band must have energy less than the least energetic  $\ell = 2$  state. For  $L = 0$ , the system becomes the true 2D electron gas.

To estimate the pressure, we further assume that the quasi-2D electron gas is a deformable jellium<sup>26–28</sup> in which the positive background charge distribution automatically deforms to cancel the electron charge distribution, making the electrostatic energy identically zero.

### C. Functionals, and Parameterizations of Exact Exchange and Correlation Energies

We have used the LDA<sup>1,5</sup>, PBE<sup>6</sup>, and SCAN<sup>7</sup> functionals to approximate the exchange-correlation energy per electron  $E_{xc}/N$  as a function of  $L/r_s^{2D}$ .

An analytic expression for  $E_x^{\text{LDA}}/N$  can be found for this system. The analytic expression was used to estimate the accuracy of the computations; this process is described in Appendix (B). This expression shows the  $L^{-1/3}$  divergence of the LDA exchange energy per electron as  $L$  tends to zero.

A Padé approximant from Betbeder-Matibet *et al.*<sup>29</sup> closely fits the known exact exchange energy per electron of a quasi-2D electron gas in the model of Eq. 2 over the whole range of  $L$ . We have employed this parametrization as our “exact” reference. The exact correlation energy per electron is known only for  $L = 0$ <sup>30</sup>. To parameterize  $E_c^{\text{exact}}/N$ , we assumed SCAN is an accurate approximation to  $E_{xc}(L = L_{\max})/N$ , and that  $E_c^{\text{exact}}/N$  depends weakly on  $L/r_s^{2D}$ . For  $a, b > 0$ , the best Padé approximant based upon known information is

$$E_c^{\text{param}}/N = -\frac{a}{1 + bL/r_s^{2D}}, \quad (12)$$

subject to the constraints

$$E_{xc}^{\text{exact}}(L = 0)/N = E_x^{\text{param}}(L = 0)/N + E_c^{\text{param}}(L = 0)/N \quad (13)$$

$$E_{xc}^{\text{SCAN}}(L = L_{\max})/N = E_x^{\text{param}}(L = L_{\max})/N + E_c^{\text{param}}(L = L_{\max})/N. \quad (14)$$

Therefore  $a = 0.0566$  and  $b = 0.351$ . As we will show in the next section, our simple parametrization for the exchange-correlation energy per electron is close to LDA, PBE, and SCAN over a wide range  $0.4L_{\max} < L < L_{\max}$ , and it is also exact at  $L = 0$ . We will therefore take this parametrization to be an “exact” reference for all quasi-2D  $L$ .

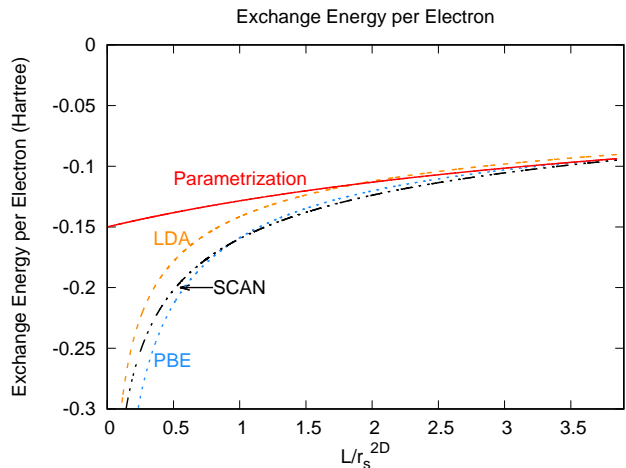


FIG. 1. (Color online) Exchange energy per electron for the model of Eq. 2 with  $r_s^{2D} = 4$ . Betbeder-Matibet *et al.*<sup>29</sup> provided the parametrization of  $E_x^{\text{exact}}/N$ .

### III. EXCHANGE-CORRELATION AND KINETIC ENERGY IN THE MODEL

As SCAN was designed to satisfy all known 17 exact constraints on a meta-GGA, we expect that the exchange and correlation energies of SCAN approach a finite value under nonuniform scaling. One can find the finite values analytically by making approximations to the ingredients of SCAN. This is demonstrated in Appendix (A) for  $E_x^{\text{SCAN}}/N$ ; for  $E_c^{\text{SCAN}}/N$ , one would follow the same procedure.

The results of the calculations of  $E_x/N$ ,  $E_c/N$  and  $E_{xc}/N = E_x/N + E_c/N$  are plotted in Figs. 1, 2, and 3 respectively. As demonstrated in previous works<sup>20,22,23</sup>, the exchange energy of LDA and of PBE diverges in the 2D limit. The correlation energy of LDA diverges, and the correlation energy of PBE tends to zero in the 2D limit, as shown previously<sup>20,22,23</sup>.

It is not apparent that  $E_{xc}^{\text{SCAN}}/N$  approaches a finite value, due to the horizontal scale of Fig. 3. To test this assumption, we fixed  $L/r_s^{2D} = 10^{-10}$  and  $r_s^{2D} = 4$ , and varied the number of integration mesh points. We observed that the numeric integration converges to a value of  $E_x^{\text{SCAN}}/N = -1.655$  Hartree in the 2D limit. The approximation in Appendix (A) finds  $E_x^{\text{SCAN}}/N = -1.671$  Hartree. Compare this to the value expected from quantum Monte Carlo (QMC) calculations<sup>30</sup>,  $E_x^{2D}/N = -0.1501$  Hartree. Thus SCAN obeys the correct nonuniform scaling limits for a functional, Eq. 9, and is about an order of magnitude in error for  $E_x/N$ . Constantin<sup>24</sup> showed that a GGA or meta-GGA would recover the correct 2D limit of the exchange energy per electron for the model of Eq. 2 if its exchange enhancement factor over LDA exchange approached  $0.521s^{-1/2}$  in this limit, in which the reduced or dimensionless density gradient  $s$  diverges. In this limit, the SCAN enhancement factor

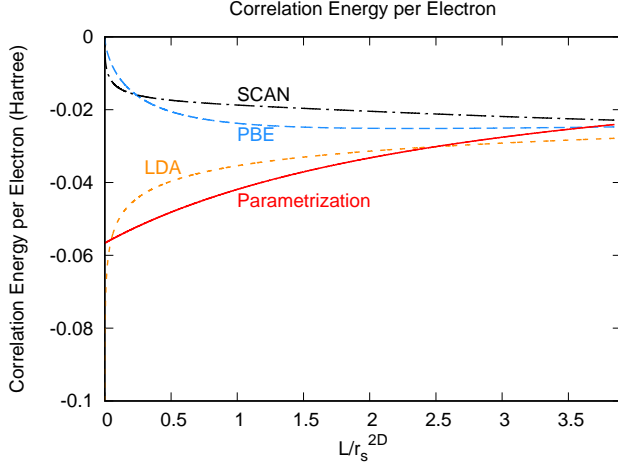


FIG. 2. (Color online) Correlation energy per electron for the model of Eq. 2 with  $r_s^{2D} = 4$ . The parametrization of  $E_c^{\text{exact}}/N$  is given by our Eq. 12.

tends to  $5.81s^{-1/2}$ , about an order of magnitude bigger. If the Constantin limit proves to be reasonably universal, it can be incorporated into a revised SCAN.

$E_c^{\text{SCAN}}/N$  tends to zero in the 2D limit, as expected by Eq. 9. This is unrealistic, but preferable to the logarithmic divergence of LDA.

Over most of the quasi-2D regime, for exchange alone (Fig. 1) and for correlation alone (Fig. 2), LDA is more accurate than PBE, and PBE is more accurate than SCAN. This surprising result reflects the challenge to density functional theory that this regime presents, although the story changes when exchange and correlation are added together.

As expected for all semilocal functionals<sup>15–17</sup>,  $E_{xc}/N$  in Fig. 3 shows a strong error cancellation between exchange and correlation, making all three functionals accurate over the wide quasi-2D range  $1.5 < L/r_s^{2D} < 3.85$ . PBE now seems to perform the worst of the three, diverging faster than LDA or SCAN as  $L/r_s^{2D} \rightarrow 0$ . We remind the reader that, while it appears LDA and SCAN both diverge,  $E_{xc}^{\text{SCAN}}/N \approx -1.655$  Hartree in the 2D limit.

The non-interacting orbital kinetic energy density, needed for meta-GGAs, is

$$\tau = \sum_{\vec{k}, |\vec{k}| < k_F^{2D}} |\nabla \phi_{1,\vec{k}}|^2 = \frac{|\nabla n|^2}{8n} + \frac{n}{2(r_s^{2D})^2} \quad (15)$$

where the first term on the right-hand side is the von Weizsäcker kinetic energy density and the second term is the true 2D kinetic energy density. As  $L \rightarrow 0$ , the first term dominates. As  $L \rightarrow 3.85r_s^{2D}$ , the integrated values per electron of the first and second terms become, in units of  $1/(r_s^{2D})^2$ , 0.333 and 0.5, respectively. Their sum becomes 0.833, not so different from the Thomas-Fermi kinetic energy 0.702 (both in units of  $1/(r_s^{2D})^2$ ).

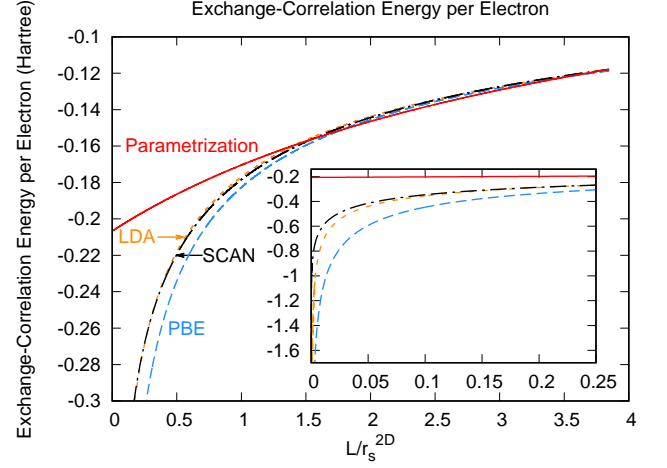


FIG. 3. (Color online) Exchange-correlation energy per electron for the model of Eq. 2 with  $r_s^{2D} = 4$ . The exact result has been parametrized as a guide to the eye. We see good error cancellation, especially for LDA and SCAN. The inset shows a closer view for  $0 < L/r_s^{2D} < 0.25$ .

#### IV. PRESSURE AND PHYSICAL INTERPRETATION OF THE MODEL

In the deformable jellium model<sup>26–28</sup>, which is consistent at the Hartree level with Eq. 2, the total energy of the electron gas inside the well is

$$E = T_s + E_{xc}, \quad (16)$$

where  $T_s = A \int_0^L dx \tau$  is the non-interacting kinetic energy per electron, and  $\tau$  is given by Eq. 15. The ratio  $(T_s + E_{xc})/T_s$  is the ratio of total to non-interacting kinetic energy. As the ratio increases, the pressure of the electron gas increases and vice versa. The ratios for the parametrized exact and SCAN values are plotted in Fig. 4. Since the non-interacting kinetic energy is treated exactly in all Kohn-Sham calculations, we can expect small relative errors in the total energy per electron from LDA, PBE and SCAN.

The thermodynamic pressure is

$$P = - \left( \frac{\partial E}{\partial V} \right)_N = - \frac{1}{A} \frac{\partial}{\partial L} (T_s + E_{xc})_{n_s^{2D}} \quad (17)$$

calculated here under the constraint of constant  $n_s^{2D}$  or  $r_s^{2D}$ . The highest pressure that can be achieved in experiment is 400 GPa from a diamond anvil<sup>31</sup>. The pressures from the parametrization and SCAN are plotted in Fig. 5. We see that 400 GPa is reached at  $L/r_s^{2D} \approx 0.6$ .

The thermodynamic pressure provides a practically-achievable lower bound to the well width. What is the pressure at the upper bound to the well width of Eq. 10? Pollack and Perdew<sup>22</sup> derived the 3D bulk Seitz radius  $r_s^{3D}$  by equating the multipole moments of the

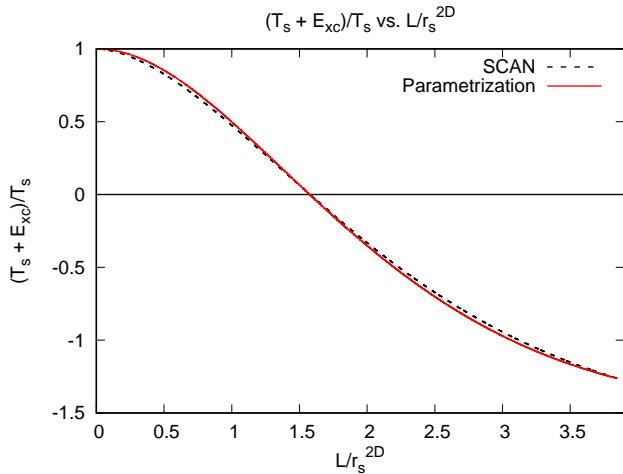


FIG. 4. (Color online) The portion of the total energy that is non-interacting kinetic energy for the model of Eq. 2, assuming the quasi-2D electron gas is a deformable jellium<sup>26–28</sup>. We compare only the SCAN and parametrized exact values.

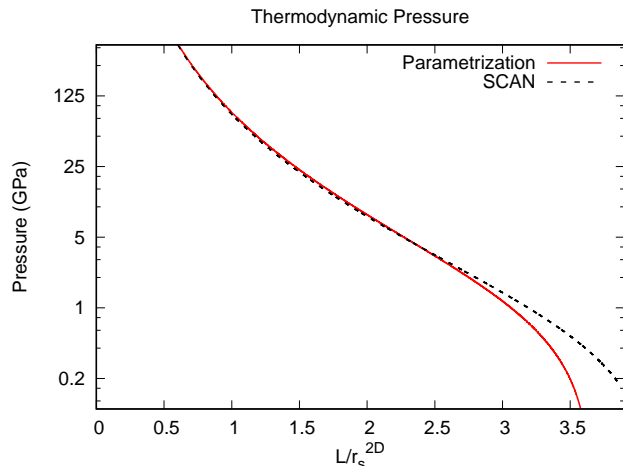


FIG. 5. (Color online) The pressure for the model of Eq. 2 found from Eq. 17, for SCAN and for the parametrized exact exchange-correlation energy in this model. The vertical axis is on a logarithmic base 5 scale, where the maximum displayed value is 400 GPa, the current upper limit of experimental pressure<sup>31</sup>.

electron density with the moments of the positive background density. We use Eq. 24 of Pollack and Perdew<sup>22</sup>

$$r_s^{3D}(L) = (3/4)^{1/3} (1 - 6/\pi^2)^{1/6} (L(r_s^{2D})^2)^{1/3} \quad (18)$$

to find  $r_s^{3D}(L = L_{\max}) = 4.87$ , nearly the same as for uncompressed metallic potassium. Thus the physical analog of our system is roughly a monolayer of potassium at equilibrium under zero or positive pressure.

A more realistic self-consistent pseudopotential calculation (but with the pressure still applied by infinite barriers) would of course produce quantitatively different re-

sults, except in the limit where  $L$  tends to zero. In this limit, the 3D electron density  $n$  tends to infinity, and the electrons behave increasingly as if they were free of all potentials other than the infinite barriers.

## V. SUMMARY AND CONCLUSIONS

We have shown that the SCAN meta-GGA is able to recover a finite  $E_x/N$  in the 2D limit of a quasi-2D electron gas. The SCAN value of  $E_x/N$  is one order of magnitude greater than the true 2D value, as found by QMC<sup>30</sup>. We did not need to use a fully-nonlocal functional to recover a finite limit.

We suspect that much of the error in the approximated exchange-correlation energy per electron at small  $L/r_s^{2D}$  is due to spurious self interaction. All semilocal functionals allow for electrons to interact with themselves<sup>32</sup>. For delocalized systems and systems of finite extent, self-interaction error is often negligible compared to the error in approximating  $E_{xc}$ . We expect that as a semi-infinite 3D system is collapsed into an infinite 2D system, and all Kohn-Sham orbitals become localized as Dirac delta functions, self-interaction errors will no longer be negligible.

As Kim *et al.*<sup>20</sup>, García-González<sup>21</sup>, and Constantin *et al.*<sup>23</sup> have shown that fully non-local functionals can recover the exact value of  $E_x/N$ , and as those functionals suffer from little to no self-interaction error, we suspect that a self-interaction correction to SCAN will increase the accuracy of  $E_x^{SCAN}/N$ .

The exact 3D exchange-correlation energy should pass over smoothly to the exact 2D exchange-correlation energy as  $L$  tends to zero. The presence of a component of interacting kinetic energy in the correlation energy, arising from electron acceleration due to mutual Coulomb repulsion, would not impede this smooth transition, since it would become increasingly confined to a two-dimensional kinetic energy in this limit. Although the general-purpose nonempirical density functionals LDA, PBE, and SCAN cannot predict the exchange-correlation energy of a true 2D electron gas, they can still in a Kohn-Sham calculation predict the total energy and pressure with a small relative error, even under extreme compression. Our simple model for the quasi-2D electron gas corresponds roughly to a monolayer of potassium under zero or positive pressure, although this physical analogy will break down at pressures so high that even the core electrons of the potassium are compressed.

## ACKNOWLEDGMENTS

The work of ADK, who co-designed the project, performed the calculations, and wrote the first draft of the manuscript, was supported by the Center for the Computational Design of Functional Layered Materials, an Energy Frontier Research Center funded by the U.S. Department of Energy, Office of Science, Basic Energy Sciences, under Grant No. DE-SC0012575, and by the Army Research Laboratory under Grant No. W91 INF-16-2-0189. The work of KW and JPP, who co-designed the project and revised the manuscript, was supported by the National Science Foundation under Grant No. DMR-1607868.

## Appendix A: Evaluation of SCAN Exchange Energy per Electron in the True 2D Limit

The 2D limit of the electron density can be found using nonuniform scaling

$$\lim_{L/r_s^{2D} \rightarrow 0} n(x) = n_s^{2D} \delta(x). \quad (\text{A1})$$

SCAN has two primary ingredients,  $s$  and  $\alpha$ ; we begin with the reduced density gradient  $s$

$$s = \frac{|\nabla n|}{2(3\pi^2)^{1/3} n^{4/3}} = \left[ \frac{\pi r_s^{2D}}{\sqrt{6}L} \right]^{2/3} \frac{|\sin(\frac{\pi x}{L}) \cos(\frac{\pi x}{L})|}{\sin^{8/3}(\frac{\pi x}{L})}. \quad (\text{A2})$$

The symmetry of the integrand permits analytic integration (see e.g. Arfken<sup>33</sup> Eq. 10.59). From Sun, Ruzsin-szky, and Perdew<sup>7</sup>,  $h_x^0 = 1.174$  and  $a_1 = 4.9479$ , and in our work  $r_s^{2D} = 4$  Bohr, thus

$$\lim_{L/r_s^{2D} \rightarrow 0} \frac{E_x^{\text{SCAN}}[n]}{N} \approx -1.671 \text{ Hartree}. \quad (\text{A7})$$

## Appendix B: Estimation of Error in Numeric Integration at any Thickness

An analytic expression for  $E_x^{\text{LDA}}/N$  at any  $L$  is<sup>1</sup>

$$\frac{E_x^{\text{LDA}}[n]}{N} = -\frac{3}{4\pi} (3\pi^2)^{1/3} \frac{A}{N} \int_0^L dx n(x)^{4/3}, \quad (\text{B1})$$

In the 2D limit,  $s(x \neq L/2) \rightarrow \infty$ , and  $s(x = L/2) \rightarrow 0$ , however the contribution from the single point  $x = L/2$  will vanish under integration. We approximate

$$\lim_{L/r_s^{2D} \rightarrow 0} s \rightarrow \infty. \quad (\text{A3})$$

The orbital kinetic energy density  $\tau$  is given by Eq. 15 and  $\alpha$  reduces to

$$\alpha = \frac{\tau - \tau^W}{\tau^{\text{unif}}} = \frac{5}{3(3\pi^2)^{2/3} (r_s^{2D})^2} n^{-2/3}. \quad (\text{A4})$$

By virtue of Eq. A1, in the 2D limit,

$$\lim_{L/r_s^{2D} \rightarrow 0} \alpha = 0. \quad (\text{A5})$$

We omit the work necessary to find the exchange energy functional integrand, and present our result for the 2D limit

$$\lim_{L/r_s^{2D} \rightarrow 0} \frac{E_x^{\text{SCAN}}[n]}{N} \approx -\frac{3}{4\pi} \frac{(3\pi^2)^{1/3}}{n_s^{2D}} h_x^0 a_1 (2(3\pi^2)^{1/3})^{1/2} \left[ \frac{2}{\pi (r_s^{2D})^2 L} \right]^2 \left[ \frac{L^2 (r_s^{2D})^2}{4} \right]^{1/2} \int_0^L dx \frac{\sin^4(\pi x/L)}{|\sin(\pi x/L) \cos(\pi x/L)|^{1/2}}. \quad (\text{A6})$$

and for the quasi-2D electron gas density, this can be reduced<sup>33</sup> to

$$\frac{E_x^{\text{LDA}}[n]}{N} = -\frac{0.566392}{r_s^{2D}} \cdot (L/r_s^{2D})^{-1/3}. \quad (\text{B2})$$

We define the percent error as

$$|E_x^{\text{analytic}} - E_x^{\text{numeric}}| / E_x^{\text{analytic}} \cdot 100\%. \quad (\text{B3})$$

For all values of  $L/r_s^{2D}$ , the percent error of our numerical LDA calculation is approximately  $1.32 \times 10^{-6}\%$ . This is a lower bound on the error for the other functionals, as the PBE and SCAN integrands can vary more rapidly as functions of  $x$  than the LDA integrand does.

- 
- <sup>1</sup> W. Kohn and L.J. Sham, Phys. Rev. **140**, A1133 (1965).
  - <sup>2</sup> J.P. Perdew and S. Kurth, in *A Primer in Density Functional Theory*, edited by C. Fiolhais, F. Nogueira, and M. Marques (Springer-Verlag, Berlin Heidelberg New York, 2003), ch. 1.
  - <sup>3</sup> J.P. Perdew and K. Schmidt, AIP Conf. Proc. **577**, 1 (2001).
  - <sup>4</sup> P. Hohenberg and W. Kohn, Phys. Rev. **136**, B864 (1964).
  - <sup>5</sup> J.P. Perdew and Y. Wang, Phys. Rev. B **45**, 13244 (1992).
  - <sup>6</sup> J.P. Perdew, K. Burke, and M. Ernzerhof, Phys. Rev. Lett. **77**, 3865 (1996).
  - <sup>7</sup> J. Sun, A. Ruzsinszky, and J.P. Perdew, Phys. Rev. Lett. **115**, 036402 (2015).
  - <sup>8</sup> J. Sun, R.C. Remsing, Y. Zhang, Z. Sun, A. Ruzsinszky, H. Peng, Z. Yang, A. Paul, U. Waghmare, X. Wu, M.L. Klein, and J.P. Perdew, Nat. Chem. **8**, 831 (2016).
  - <sup>9</sup> J.W. Furness, Y. Zhang, C. Lane, I.G. Buda, B. Barbiellini, R.S. Markiewicz, A. Bansil, and J. Sun, Nat. Comm. Phys. **1**, 11 (2018).
  - <sup>10</sup> A. Patra, J.E. Bates, J. Sun, and J.P. Perdew, Proc. Nat. Acad. Sci. U.S.A., E9181 (2017).
  - <sup>11</sup> M. Chen, H.-Y. Ko, R.C. Remsing, M.F.C. Andrade, B. Santra, Z. Sun, A. Selloni, R. Car, M.L. Klein, J.P. Perdew, and X. Wu, Proc. Nat. Acad. Sci. U.S.A. **114**, 10847 (2017).
  - <sup>12</sup> Y. Zhang, D.A. Kitchaev, J. Yang, T. Chen, S.T. Dacek, R.A. Sarmiento-Pérez, M.A.L. Marques, H. Peng, G. Ceder, J.P. Perdew, and J. Sun, npj Computational Materials **4**, 9 (2018).
  - <sup>13</sup> C. Shahi, J. Sun, and J.P. Perdew, Phys. Rev. B **97**, 094111 (2018).
  - <sup>14</sup> K. Burke and J.P. Perdew, Int. J. Quantum Chem. **56**, 199 (1995).
  - <sup>15</sup> K. Burke, J.P. Perdew, and D.C. Langreth, Phys. Rev. Lett. **73**, 1283 (1994).
  - <sup>16</sup> K. Burke, J.P. Perdew, and M. Ernzerhof, J. Chem. Phys. **109**, 3760 (1998).
  - <sup>17</sup> O. Gunnarsson and B.I. Lundqvist, Phys. Rev. B **13**, 4274 (1976).
  - <sup>18</sup> A. Görling and M. Levy, Phys. Rev. A **45**, 1509 (1992).
  - <sup>19</sup> J.C. Ryan, Phys. Rev. B **43**, 4499 (1991).
  - <sup>20</sup> Y.-H. Kim, I.-H. Lee, S. Nagaraja, J.-P. Leburton, R.Q. Hood, and R.M. Martin, Phys. Rev. B **61**, 5202 (2000).
  - <sup>21</sup> P. García-González, Phys. Rev. B **62**, 2321 (2000).
  - <sup>22</sup> L. Pollack and J.P. Perdew, J. Phys. Condens. Matter **12**, 1239 (2000).
  - <sup>23</sup> L.A. Constantin, J.P. Perdew, and J. M. Pitarke, Phys. Rev. Lett. **101**, 016406 (2008).
  - <sup>24</sup> L.A. Constantin, Phys. Rev. B **78**, 155106 (2008).
  - <sup>25</sup> D.M. News, Phys. Rev. B **1**, 3304 (1970).
  - <sup>26</sup> J.W. Allen and S.A. Rice, J. Chem. Phys. **67**, 5105 (1977).
  - <sup>27</sup> M. Koskinen, P.O. Lipas, and M. Manninen, Z. Phys. D: At., Mol. Clusters **35**, 285 (1995).
  - <sup>28</sup> H.T. Tran and J.P. Perdew, Am. J. Phys. **71**, 1048 (2003).
  - <sup>29</sup> O. Betbeder-Matibet, M. Combescot, and C. Tanguy, Phys. Rev. B **53**, 12929 (1996).
  - <sup>30</sup> Y. Kwon, D.M. Ceperley, and R.M. Martin, Phys. Rev. B **48**, 12037 (1993).
  - <sup>31</sup> B. Li, C. Ji, W. Yang, J. Wang, K. Yang, R. Xu, W. Liu, Z. Cai, J. Chen, and H.-k. Mao, Proc. Nat. Acad. Sci. U.S.A. **115**, 1713 (2018).
  - <sup>32</sup> J.P. Perdew and A. Zunger, Phys. Rev. B **23**, 5048 (1981).
  - <sup>33</sup> G. Arfken, *Mathematical Methods for Physicists* (Academic, San Diego, 1985), p. 560.